

UNCLASSIFIED

SECURITY CLASSIFICATION OF THIS PAGE

AD-A201 136

## REPORT DOCUMENTATION PAGE

Form Approved  
OMB No 0704-0188  
Exp Date Jun 30, 1986

1a REPORT SECURITY CLASSIFICATION UNCLASSIFIED		1b RESTRICTIVE MARKINGS	
2a SECURITY CLASSIFICATION AUTHORITY		3 DISTRIBUTION / AVAILABILITY OF REPORT Approved for public release; distribution unlimited.	
2b DECLASSIFICATION / DOWNGRADING SCHEDULE			
4 PERFORMING ORGANIZATION REPORT NUMBER(S) HDL-TR-2151		5 MONITORING ORGANIZATION REPORT NUMBER(S)	
6a. NAME OF PERFORMING ORGANIZATION Harry Diamond Laboratories	6b OFFICE SYMBOL (if applicable) SLCHD-ST-SS	7a NAME OF MONITORING ORGANIZATION	
6c. ADDRESS (City, State, and ZIP Code) 2800 Powder Mill Road Adelphi, MD 20783-1197		7b ADDRESS (City, State, and ZIP Code)	
8a. NAME OF FUNDING / SPONSORING ORGANIZATION U.S. Army Laboratory Command	8b OFFICE SYMBOL (if applicable) AMSLC	9 PROCUREMENT INSTRUMENT IDENTIFICATION NUMBER	
8c. ADDRESS (City, State, and ZIP Code) 2800 Powder Mill Road Adelphi, MD 20783-1145		10 SOURCE OF FUNDING NUMBERS	
		PROGRAM ELEMENT NO P61102.H44	PROJECT NO AH44
		TASK NO	WORK UNIT ACCESSION NO
11. TITLE (Include Security Classification) High-Frequency Modulation and Fiber-Optic Links for Phased Arrays			
12. PERSONAL AUTHOR(S) Fred Semendy and Emanuel Katzen			
13a TYPE OF REPORT Final	13b TIME COVERED FROM 8/87 TO 3/88	14 DATE OF REPORT (Year, Month, Day) October 1988	15. PAGE COUNT 20
16. SUPPLEMENTARY NOTATION HDL project: AE17L1, AMS code: 611102.H44			
17. COSATI CODES		18. SUBJECT TERMS (Continue on reverse if necessary and identify by block number)	
FIELD	GROUP	SUB-GROUP	
17	8		
		High-frequency modulation, fiber optics, direct modulation, external modulation, laser diodes, detectors, phased array	
19. ABSTRACT (Continue on reverse if necessary and identify by block number)			
<p>Direct modulation and detection studies were performed using various laser diodes from 2 to 22 GHz. A <math>\text{LiNbO}_3</math> travelling wave Mach-Zehnder interferometer was used for external modulation. The modulated beams were coupled into an optical fiber, demodulated by fast detectors, and spectrum analyzed. Attempts were also made to obtain higher order harmonics after direct modulation of the laser diodes by making use of the nonlinear behavior of the lasers. However, very high frequencies beyond K band could not be detected because of the limitations of the detectors.</p>			
20 DISTRIBUTION / AVAILABILITY OF ABSTRACT <input checked="" type="checkbox"/> UNCLASSIFIED/UNLIMITED <input type="checkbox"/> SAME AS RPT <input type="checkbox"/> DTIC USERS		21 ABSTRACT SECURITY CLASSIFICATION UNCLASSIFIED	
22a. NAME OF RESPONSIBLE INDIVIDUAL Fred Semendy		22b TELEPHONE (Include Area Code) (202) 394-4160	22c OFFICE SYMBOL SLCHD-ST-SS

## CONTENTS

	Page
1. INTRODUCTION .....	5
2. EXPERIMENTAL SETUP .....	6
3. RESULTS AND DISCUSSION .....	10
4. CONCLUSIONS .....	14
REFERENCES .....	15
DISTRIBUTION .....	17

## FIGURES

1. Experimental setup for microwave fiber-optic link--direct modulation .....	6
2. Experimental setup for external modulation .....	8
3. Guided-wave Mach-Zehnder interferometric modulator .....	8
4. Analog modulation of optical output by modulation of bias current ...	9
5. Noise level versus bias current for 4-GHz modulation and photodetector current versus bias current .....	11
6. Detected signal after demodulation for various frequencies .....	12
7. Power spectrum of baseband and harmonics of a directly modulated laser .....	13
8. Power level obtained by external modulation .....	13



Accession For	
NTIS GRA&I	<input checked="" type="checkbox"/>
DTIC TAB	<input type="checkbox"/>
Unannounced	<input type="checkbox"/>
Justification	
By _____	
Distribution/	
Availability Codes	
Dist	Avail and/or Special
A-1	

## 1. INTRODUCTION

A phased-array antenna is a type of microwave antenna with a number of individual radiating elements [1] placed regularly on the antenna surface. Typical element spacings are about a wavelength, and for the best performance from the array, each element needs to be accurately controlled. Depending upon the system applications, arrays can vary from tens to thousands of elements. Higher frequency systems will require smaller array dimensions. A modular approach with amplification, control, and distribution of signals can provide cost-effective array systems with easier manipulation.

A good solution to the distribution problem is the use of fiber-optic technology. It is believed that fiber optics has several advantages for distribution of signals. Optical fibers have large bandwidth, which is a useful capability for high-frequency transmission. They are also characterized by low dispersion, low loss, immunity from electromagnetic interference, and low cross talk [2]. Recent advances in semiconductor laser diode technology have helped to achieve high-frequency modulation, and interaction with solid-state microwave devices has demonstrated the possibility of fiber-optic links and delay lines, phased-array beam steering, and microwave power control. Modulation of the optical source is feasible either by directly modulating the laser bias current or by using an external electro-optic modulator. Direct modulation and fiber-optic coupling have been done by a number of people including Bechtle and Siegel [3], a fiber-optic link to a 1.1-km fiber has been described by Pan [4], a 10.3-GHz bandwidth link was demonstrated by Lau et al [5], and a 12.5-GHz bandwidth link was shown by Su et al [6]. Recently Olshansky [7] achieved a bandwidth of 22 GHz after directly modulating an InGaAsP laser. Work also has been done by Herczfeld et al, Daryoush et al, and Goldberg et al [8-10]. Most of these studies include optical injection locking or harmonic injection locking.

External modulation has also been demonstrated with a variety of electro-optic devices at frequencies up to 17 GHz [11,12]. The external modulation is performed by an rf signal imposed on the optical wave, which is input from the laser diode through a fiber pigtail. These electro-optic devices are fabricated using  $\text{LiNbO}_3$ , and in the simplest analysis an optical waveguide in  $\text{LiNbO}_3$  follows the same principle as waveguides in silica (that is, optical fibers). Light will propagate in the core region as long as the angle of incidence is greater than the critical angle. For this the index of refraction of the waveguide region should be greater than that of  $\text{LiNbO}_3$ .

In this work, modulation studies were performed by directly modulating the bias current to various laser diodes from 2 to 22 GHz and also externally modulating a laser beam using an  $\text{LiNbO}_3$  travelling-wave Mach-Zehnder modulator. The modulated beams were coupled into an optical fiber and demodulated by appropriate detectors. Demodulated signals were analyzed by spectrum analyzers. The characteristics of the various components of microwave fiber-optic links at 0.83 and 1.3  $\mu\text{m}$  are discussed. Emphasis is on problems relating to the choice of components and to optimizing the link signal-to-noise ratio. Attempts were also made to obtain the higher order harmonics after directly modulating a 0.83- $\mu\text{m}$  laser by making use of the non-linear behavior of the laser diode.

## 2. EXPERIMENTAL SETUP

The arrangement for the direct modulation experiment is shown in figure 1. The setup consists of a laser diode, bias tees, multimode or single-mode fiber, fast detectors, an amplifier, objective lenses, and a spectrum analyzer.

Laser diode.--A Mitsubishi ML 2701 AlGaAs window structure laser emitting light around  $0.83\text{ }\mu\text{m}$  was used for low-frequency modulation, and a GTE vapor-phase-regrown buried heterostructure (VPR-BH) InGaAsP  $1.3\text{-}\mu\text{m}$  semiconductor laser was used for high-frequency modulation.

Bias tees.--The bias tees used were either an HP 33150 type for low-frequency modulation or an HP 11612A type for high-frequency modulation. These bias tees have extremely broad bandwidth with good port match and low insertion loss. The bias networks provide dc bias to the center conductor of a coaxial line which can be connected to the devices under test while blocking dc bias from the rf circuit.

Multimode fiber.--Multimode fibers made by Corning were used for the coupling. The fibers were  $50/125\text{ }\mu\text{m}$  size (that is,  $50\text{-}\mu\text{m}$  core,  $125\text{ }\mu\text{m}$  with cladding), about 2 km long, and rated for 2 dB/km loss.

Fast detectors.--For low-frequency detection at  $0.83\text{ }\mu\text{m}$ , Mitsubishi PD 1000 series Si avalanche photodiodes were used. These detectors have high-speed response, low multiplication noise, and high gain bandwidth, with a breakdown voltage of 120 V. For high-frequency detection at  $1.3\text{ }\mu\text{m}$ , an ultra-high-speed InGaAs photodiode made by GTE was used [13]. These photodiodes are

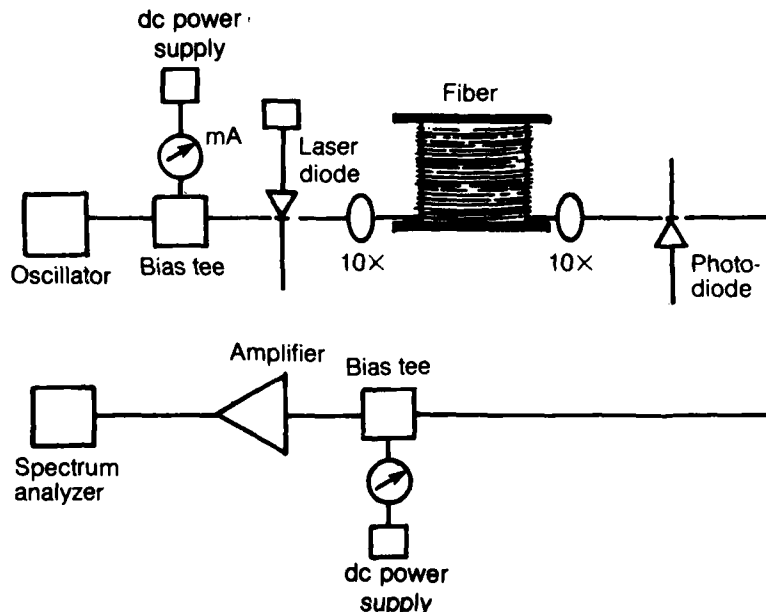


Figure 1. Experimental setup for microwave fiber-optic link--direct modulation.

substrate-illuminated InGaAs PIN mesa structures that achieve low capacitance and short transit time without sacrificing responsivity. The photodiode material consists of a 3- $\mu\text{m}$  InP buffer layer, and a 1.2- $\mu\text{m}$  InGaAs absorption layer, both grown by liquid phase epitaxy on an n+ InP substrate. A Cd-diffused p-n junction was placed at a depth of 0.5  $\mu\text{m}$  below the InGaAs surface. Mesas having a 40- $\mu\text{m}$  diameter were formed by wet chemical etching, and an aperture was opened in the inside metallization for substrate-side illumination. The detector is mounted at the open laboratory package, and microstrip was coupled to an SMA-compatible Willstron K-connector. For low-frequency detection at 1.3  $\mu\text{m}$ , a Mitsubishi PD 7005 photodetector was used. This InGaAs photodiode is designed to operate in the 1.0 to 1.6  $\mu\text{m}$  range with performance superior to a germanium photodiode in quantum efficiency and dark current.

Amplifier.--For signal amplification after detection, an AvanteK AMT 8035 with gain of about 50 dB, a noise figure of 3.5 dB, and power output of +15 dBm was used for 0.83  $\mu\text{m}$ . At 1.3  $\mu\text{m}$  the amplification was carried out using an AvanteK AMT 2035 amplifier with a gain of 26 dB, noise figure of 7 dB, and power output of +17 dBm. Power measurements were done before and after using amplifiers.

The experimental setup for the external modulation based fiber-optic link is shown in figure 2. A General Optics 1.3- $\mu\text{m}$  laser diode was used as the optical source. A Crystal Technology model MZ 313 optical guided-wave Mach-Zehnder (OGW-MZ) high-speed intensity modulator was used for the external modulation. This  $\text{LiNbO}_3$ -based electro-optic modulator has a bandwidth of 3 GHz for a drive voltage of 8 V with an extinction ratio of 20 dB minimum. This Mach-Zehnder interferometer is a highly developed waveguide device, as shown in figure 3. The intensity output depends on the effective path length of the two branches. The input light is split at the y-junction, and the two portions travel in the interferometer branches, combining at the other end to form the output signal. When a voltage is applied in one branch through the mounted electrode, the light velocity changes in that branch because of the changes in the linear electro-optic effect. This will change the relative phase between the two branches at the output y-junction which is detected. These interferometers are relatively efficient intensity modulators. The output from the modulator was coupled into a 1.3- $\mu\text{m}$ -wavelength fiber and detected, amplified, and analyzed using the spectrum analyzer.

One of the advantages of a laser diode is that it can not only be coupled to an optical fiber but also directly modulated. Generally, above lasing threshold, the output from a laser is linear as a function of injection current. The analysis shows that the modulation response has the transfer characteristics of a second-order low-pass network [14]. A relaxation oscillation in the laser occurs, which is at the resonance modulation response. This resonance is the result of the interplay between the optical field and population inversion, and its strength depends on the spontaneous emission factor, lateral carrier diffusion, and presence of saturable absorbing defects. From small-signal analysis we get

$$f_T = \frac{1}{2\pi} \left( \frac{AP_0}{\tau_p} \right)^{1/2}, \quad (1)$$

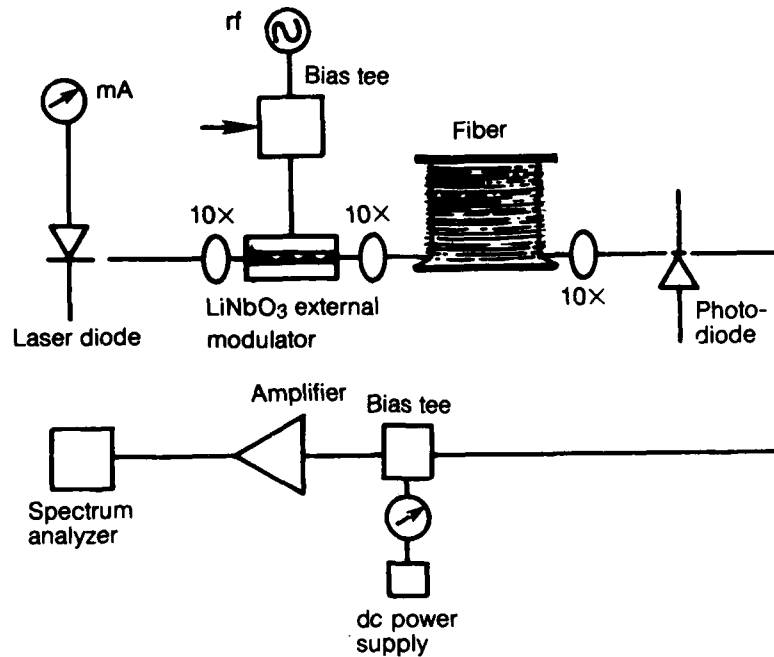
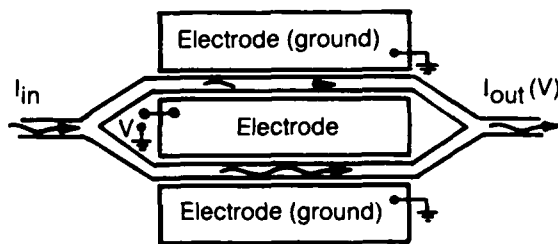


Figure 2. Experimental setup for external modulation.

Figure 3. Guided-wave Mach-Zehnder interferometric modulator.



where  $\tau_p$  is the photon lifetime (given by  $\tau_p = (1/\gamma)[\alpha + (1/\gamma)\ln(1/R)]$ , where  $\gamma$  is the group velocity of light,  $\alpha$  is the distributed loss,  $L$  is the length of the cavity, and  $R$  is the mirror reflectivity),  $P_0$  is the steady-state photon density, and  $A$  is the differential gain constant. The modulation bandwidth of the laser is equal to  $f_T$ .

The waveform is slightly distorted from the normal for high-frequency modulation. In the above equation  $\tau_p$  can be reduced by shortening the laser cavity, and  $P_0$ , the photon density, can be increased by increasing bias current. Low-frequency modulation is equivalent to ramping the laser up and down along the current/light curve adiabatically, as shown in figure 4. A limiting factor is the higher junction temperature generated by the increased current density resulting from a shorter cavity. The differential gain can be increased by the operating laser at low temperature, but for practical reasons, the lasers were operated near room temperature using an automatic temperature controller.

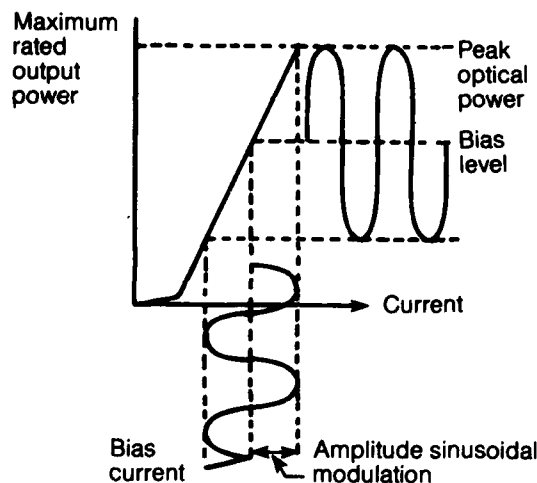


Figure 4. Analog modulation of optical output by modulation of bias current.

The nonlinear modulation of the semiconductor laser can also be performed to achieve high frequencies for phased arrays. In this technique, the nonlinearity of the laser is taken advantage of, and large-signal modulation is performed to produce distortions, thus enhancing the harmonic content [15,16]. The substantial increase in harmonic levels occurs at frequencies corresponding to the large-signal relaxation oscillation frequency, given by [17]

$$\omega = \omega_T \frac{2I_1(a)}{I_0(a)} = \omega_T \phi(a) , \quad (2)$$

where  $\omega_T = 2\pi f_T$  is the small-signal relaxation oscillation frequency,  $I_k(x)$  is the modified Bessel function of the first kind and order  $k$ , and  $a$  is the amplitude of photon density. This amplitude is related to the optical modulation depth,  $m$ , by [18]

$$m = a \left\{ \left[ \frac{\Omega^2}{\Omega_T^2} - \frac{\phi}{a} \right]^2 + \Omega^2 \tau_p^2 \left[ 1 + \left( \Omega_T^2 \tau_p \tau_s \right)^{-1} \right] \right\}^{1/2} , \quad (3)$$

where  $\tau_s$  is the electron lifetime. Even though the second harmonic could be obtained for the low-frequency (4-GHz) modulation, for high frequency (21 GHz) the harmonics could not be obtained because of a lack of the proper components.

Direct modulation has advantages in its simplicity and lower power requirements. But for external modulation the requirements for both high-frequency response and low noise can be satisfied by the same laser. Since in this case the laser current is not modulated, the external modulation is free from direct interaction of the rf modulation signal with the low-frequency

laser noise components and relaxation resonance. For the external modulator with a 3-dB bandwidth of 3 GHz, the modulation transfer function is given by

$$P = P_{pk} \sin^2\left(\frac{\pi V}{2V_{\pi}} + \phi\right), \quad (4)$$

where  $V_{\pi}$  is the half-wave voltage, which depends on the dimensions and material of the modulator. The modulator is typically biased to  $\phi = \pm\pi/4$  for linear modulation.

### 3. RESULTS AND DISCUSSION

Direct modulation of the laser current was accomplished up to 22 GHz for the laser diode, and the laser current was successfully coupled to an optical fiber and detected. Indications are that noise will increase for higher frequencies of modulation.

In the direct modulation link, the rf power was coupled into the laser using a bias tee as indicated earlier. The bias to the laser (at about 36 mA) was supplied through a steady current power supply. The laser was modulated around 4 GHz with 8 dBm rf incident power, and both signal and noise level changes were measured by changing the bias current. A digital meter was used to monitor the photodetector for the detection current level. The demodulated optical power at the output of the fiber line was 0.5 to 2.5 mW for the bias currents of 20 to 45 mA used. The threshold current typically was found to be about 18 mA. Figure 5 gives the noise level and detector current for various bias currents.

As indicated in the figure, the noise level is increasing, and the loss in the power is due to the conversions to and from the optical signal added to the optical propagation loss. Most of the power loss as seen by the output measurement is due to matching circuit loss, efficiency at one face, laser fiber coupling loss, fiber loss, and fiber detector coupling loss. Also the load and source impedance should be taken into consideration along with amplifier gain. The detector is a square-law device which converts the incident optical signal into a current. The optical losses have a greater impact on the link loss than any other type of loss. Generally the insertion loss is dominated by the laser external differential efficiency for one facet and laser fiber coupling. However, this can be greatly offset by using the amplifier with appropriate gain.

For the ultra-high-frequency modulation, the GTE InGaAsP laser diode was set up as shown in figure 1. This laser has a cavity length of 100  $\mu\text{m}$ . For heat dissipation, the microstrip line was fabricated on a BeO substrate. A microwave fiber-optic link study was carried out by direct modulation of this laser, coupling to an optical fiber, and demodulation with an ultra-fast detector, as explained earlier. The direct modulation of the laser current was accomplished by 15- to 21-GHz signals with leveled power of 10 dBm on the 80-mA laser current [19]. There was a loss of 5 dBm in the coaxial cables. The spectrum analysis was done with a resolution bandwidth of 1 MHz, video bandwidth of 100 kHz, sweep time of 300 ms, and attenuation of 10 dB. Various modulated results are given in figure 6.

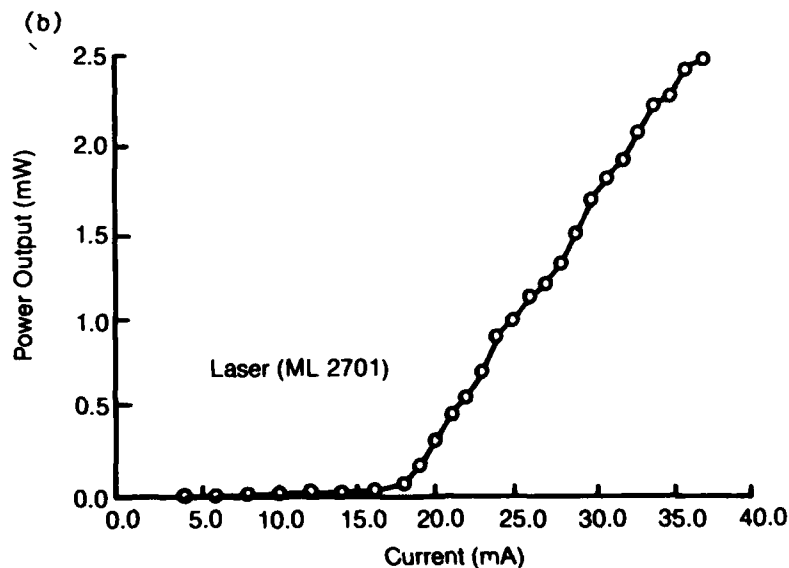
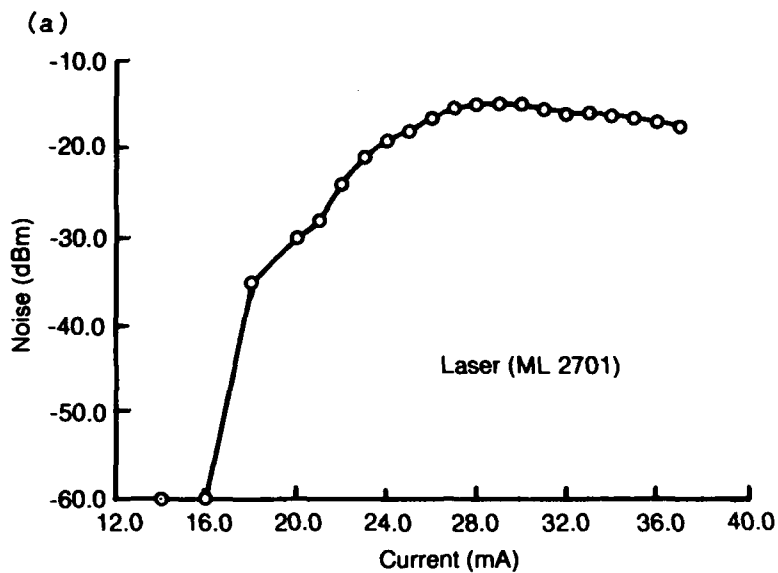


Figure 5. (a) Noise level versus bias current for 4-GHz modulation and (b) photodetector current versus bias current.

The demodulated signals were measured, detected, and analyzed after amplification by two low-noise amplifiers. There is a gradual power level change which can be attributed to the limitation of the laser diode, amplifiers, and coaxial cables. Even though much higher frequency modulation would have been possible, this was not done because of a lack of microwave generators and other required components.

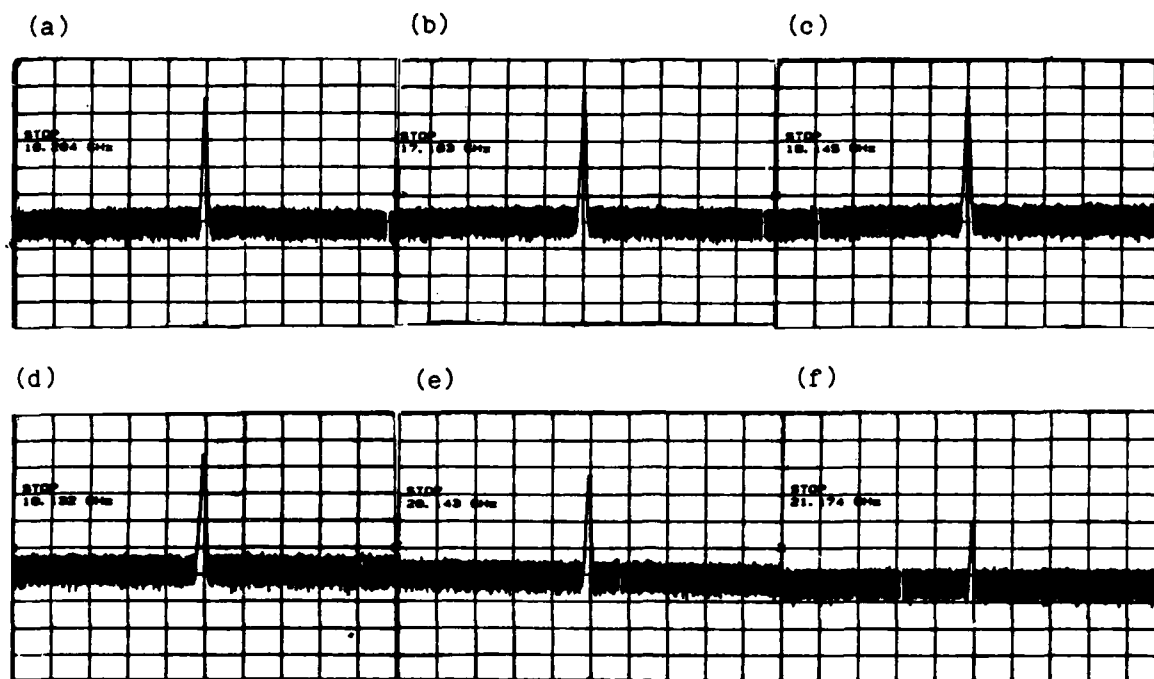


Figure 6. Detected signal after demodulation for various frequencies:  
 (a) 16-GHz modulation; (b) 17-GHz modulation; (c) 18-GHz modulation;  
 (d) 19-GHz modulation; (e) 20-GHz modulation; and (f) 21-GHz modulation.

The room-temperature modulation of laser diodes beyond 22 GHz was not attempted at the present time. But there is reasonable interest in designing phased arrays and other fiber-optic systems in the millimeter-wave region. For this purpose, the nonlinearities of the laser can be taken advantage of to extend modulation frequencies to the millimeter-wave region. Large-signal modulation of lasers causes distortion and increases the harmonic content [20]. A well-behaved laser shows very little nonlinear distortion at low frequencies of modulation. This is because the laser is virtually in a quasi-steady state as it is ramping up and down along the light/current curve, and the linearity is basically that of the cw light/current characteristics. However, the harmonic distortions increase rapidly at modulation frequencies greater than 1 GHz, and the second and higher harmonics show up as indicated in figure 7.

These results can be explained by a perturbative analysis of the laser rate equations which indicates that the fluctuations of electrons and photons cause the large harmonic distortions observed at high frequencies. Even though we see an increase in the power level for the second harmonic, for the higher orders the power levels seem to decrease.

The optical spectrum obtained by external modulation is given in figure 8. This spectrum was obtained with center frequencies of 300 and 500 MHz with a resolution bandwidth of 10 kHz. The 3-dB link frequency could be increased

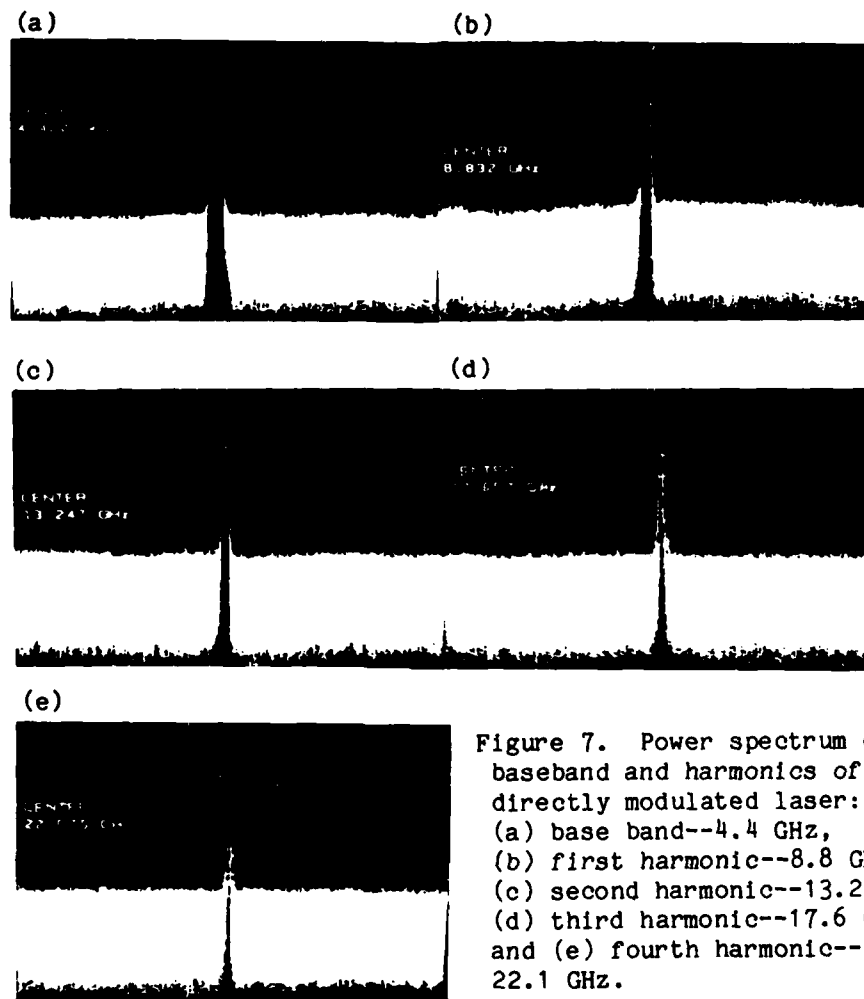


Figure 7. Power spectrum of baseband and harmonics of a directly modulated laser:  
 (a) base band--4.4 GHz,  
 (b) first harmonic--8.8 GHz,  
 (c) second harmonic--13.2 GHz,  
 (d) third harmonic--17.6 GHz,  
 and (e) fourth harmonic--22.1 GHz.

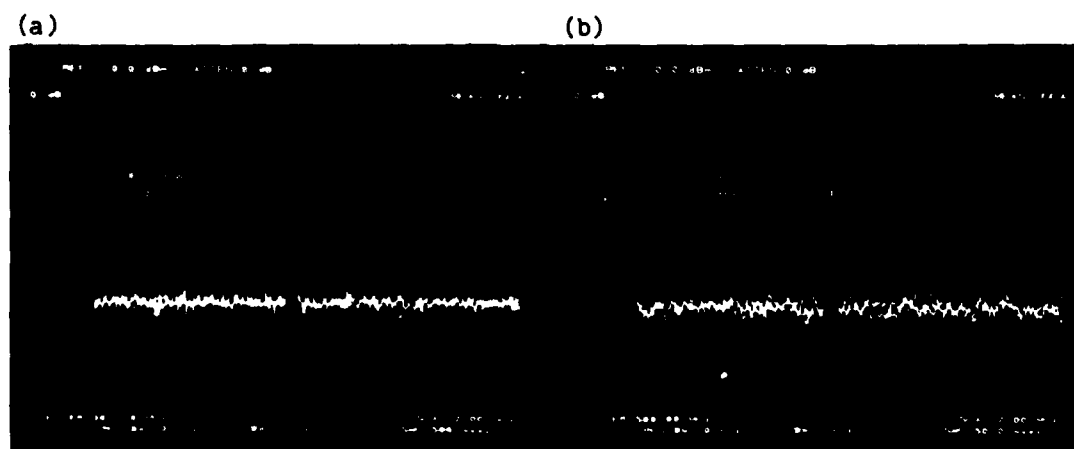


Figure 8. Power level obtained by external modulation: (a) 300 MHz and (b) 500 MHz.

to 3 GHz because the power of the rf generator was low. The laser power was about 2 mW and the rf drive power was close to 300 mW. The insertion loss of the link can be calculated knowing the input/output rf power levels, the gain of the amplifier, and the source and load impedance. Calculations indicate substantially greater loss in the external modulation link; however, this loss can be overcome by increasing optical power. The nonlinearity factor in the external modulation studies was not considered. The nonlinear source will be the external modulator and any preamplifier used in the link system. For a high modulation index, the power preamplifier has to be driven near the 1-dB compression point. In the Mach-Zehnder modulator the nonlinearities are caused by the large-signal optic-intensity/voltage-response relationship.

#### 4. CONCLUSIONS

We have demonstrated the operation of a microwave fiber-optic link in the  $K_u$  band and beyond by direct modulation. We also attempted to understand and analyze the nonlinearities of the laser diodes which generate harmonics. In particular, a laser diode was directly modulated and fiber optically linked, and the harmonics were analyzed up to 22 GHz. Because high-bandwidth laser diodes are unavailable, this perhaps is a better way to obtain very high frequencies. No attempts were made to study the harmonics of the 1.3- $\mu$ m InGaAsP laser with the base band at 21 GHz. Theoretically it is possible to obtain frequencies at 42, 63, 84, and 105 GHz with proper cables (waveguides), detectors, amplifiers, and spectrum analyzers. However, at present appropriate detectors and amplifiers are not available for demodulation and amplification at such high frequencies. Direct modulation offers simplicity, low drive power, and low link loss.

With the external modulator, the modulation frequency was limited to 500 MHz because of a lack of sufficient rf power. External modulation relaxes the demand for high-frequency lasers and gives some flexibility in choosing low-noise lasers. The above two modulation/demodulation studies show the capability and feasibility of a microwave fiber-optic link system at high frequencies.

## REFERENCES

1. M. I. Skolnik, Introduction to Radar Systems, 2nd Edition, McGraw Hill (1982).
2. P. K. Wahi, Optics for Microwave Applications, IEEE MTT-S Digest (1985), 295.
3. D. W. Bechtle and S. A. Siegel, An Optical Communications Link in the 2.0-6.0 GHz Band, RCA Review 43 (1982), 277.
4. J. J. Pan, 5-GHz Wide-Band Fiber Optic Link, Digest of Technical Papers, IEEE/OSA Optical Fiber Communications Conference, New Orleans, LA (February 1983).
5. K. Y. Lau, N. Bar-Chaim, I. Ury, and A. Yariv, An 11 GHz Direct Modulation Bandwidth GaAlAs Window Laser on Semi-insulating Substrate Operating at Room Temperature, Appl. Phys. Lett. 45 (1984), 316.
6. C. B. Su, V. Lanziera, W. Powaziniak, E. Meland, R. Olshansky, and R. B. Lauer, 12.5 GHz Direct Modulation Bandwidth of Vapor Phase Regrown 1.3  $\mu$ m InGaAsP Buried Heterostructure Laser, Appl. Phys. Lett. 46, No. 4 (1985), 344.
7. R. Olshansky, W. Powaziniak, P. Hill, V. Lanziera, and R. B. Lauer, InGaAsP Buried Heterostructure Laser with 22 GHz Bandwidth and High Modulation Efficiency, Electron. Lett. 213, No. 16 (1987), 839.
8. P. R. Herczfeld, A. S. Daryoush, A. Rosen, A. K. Sharma, and V. M. Contario, Indirect Subharmonic Optical Injection Locking of a Millimeter-Wave IMPATT Oscillator, IEEE Trans. Microwave Theory Tech. MTT-34, No. 12 (1986), 1371.
9. A. S. Daryoush, P. R. Herczfeld, Z. Turki, and P. K. Wahi, Comparison of Indirect Optical Injection-Locking Techniques of Multiple X-Band Oscillators, IEEE Trans. Microwave Theory Tech. MTT-34, No. 12 (1986), 1363.
10. L. Goldberg, H. F. Taylor, and J. F. Weller, Microwave Signal Generation with Injection-Locked Laser Diodes, Electron. Lett. 19, No. 13 (1983), 491.
11. C. M. Gee and G. D. Thurmond, High Speed Integrated Optics Travelling Wave Modulator, Proceedings, 2nd European Conference on Integrated Optics, (1983), 118.
12. C. M. Gee, G. D. Thurmond, and H. M. Yen, 17 GHz Bandwidth Electro-Optic Modulator, Appl. Phys. Lett. 43, No. 11 (1983), 998.
13. J. Schlafer, C. B. Su, W. Powaziniak, and R. B. Lauer, 20 GHz Bandwidth InGaAs Photodetector for Long-Wavelength Microwave Optical Links, Electron. Lett. 21, No. 11 (1985), 469.

14. K. Y. Lau and A. Yariv, Ultra-High Speed Semiconductor Lasers, IEEE J. Quantum Electron. 21, No. 2 (1985), 121.
15. H. Kressel and J. K. Butler, Semiconductor Laser and Heterojunction LEDs, Academic Press, New York (1979).
16. T. Ikegami and Y. Suematsu, Large-Signal Characteristics of Directly Modulated Semiconductor Injection Lasers, Electron. Comm. Jpn. B 53, No. 69 (1970), 69.
17. A. S. Daryoush, Large-Signal Modulation of Laser Diodes and its Applications in Indirect Optical Injection Locking of the Millimeter Wave Oscillators, Ph.D. Dissertation, 1986, Drexel University, Philadelphia, PA.
18. R. A. Kiel, Behavior and Dynamics of Optically Controlled TRAPPATT Oscillators, IEEE Trans. Electron Devices ED-25 (1978), 703.
19. F. Semendy and E. Katzen, Microwave Fiberoptic Links for Phased Arrays, SPIE Proceedings, Los Angeles (January 1988).
20. K. Lau and A. Yariv, Intermodulation Distortion in a Directly Modulated Semiconductor Injection Laser, Appl. Phys. Lett. 45, No. 10 (1984), 1034.

DISTRIBUTION

ADMINISTRATOR  
DEFENSE TECHNICAL INFORMATION  
CENTER  
ATTN DTIC-DDA (12 COPIES)  
CAMERON STATION, BUILDING 5  
ALEXANDRIA, VA 22314

DIRECTOR  
DEFENSE ADVANCED RESEARCH  
PROJECTS AGENCY  
ATTN J. FRIEBELE  
1400 WILSON BLVD  
ARLINGTON, VA 22209

DIRECTOR  
DEFENSE NUCLEAR AGENCY  
ATTN TECH LIBRARY  
WASHINGTON, DC 20305

UNDER SECRETARY OF DEFENSE RES  
& ENGINEERING  
ATTN TECHNICAL LIBRARY, 3C128  
WASHINGTON, DC 20301

OFFICE OF THE ASSIST SEC  
OF THE ARMY (RDA)  
ATTN DAMA-ARZ-A, CHIEF SCIENTIST,  
L. CAMERON  
ATTN DAMA-ARZ-B, I. R. HERSHNER  
WASHINGTON, DC 20310

COMMANDER  
US ARMY ARMAMENT MUNITIONS &  
CHEMICAL COMMAND (AMCCOM)  
US ARMY ARMAMENT RESEARCH &  
DEVELOPMENT CENTER  
ATTN DRDAR-TSS, STINFO DIV  
DOVER, NJ 07801

COMMANDER  
ATMOSPHERIC SCIENCES LABORATORY  
ATTN TECHNICAL LIBRARY  
WHITE SANDS MISSILE RANGE, NM  
88002

DIRECTOR  
US ARMY BALLISTIC RESEARCH  
LABORATORY  
ATTN SLCBR-DD-T (STINFO)  
ABERDEEN PROVING GROUND, MD  
21005

DIRECTOR  
US ARMY ELECTRONICS WARFARE  
LABORATORY  
ATTN J. CHARLTON  
ATTN DELET-DD  
FT MONMOUTH, NJ 07703

COMMANDING OFFICER  
USA FOREIGN SCIENCE &  
TECHNOLOGY CENTER  
FEDERAL OFFICE BUILDING  
ATTN DRXST-BS, BASIC SCIENCE  
DIV  
CHARLOTTESVILLE, VA 22901

COMMANDER  
US ARMY MATERIALS & MECHANICS  
RESEARCH CENTER  
ATTN DRXMR-TL, TECH LIBRARY  
WATERTOWN, MA 02172

US ARMY MATERIEL COMMAND  
5001 EISENHOWER AVE  
ALEXANDRIA, VA 22333-0001

COMMANDER  
US ARMY MISSILE & MUNITIONS  
CENTER & SCHOOL  
ATTN ATSK-CTD-F  
ATTN DRDMI-TB, REDSTONE SCI  
INFO CENTER  
REDSTONE ARSENAL, AL 35809

DIRECTOR  
NIGHT VISION & ELECTRO-OPTICS  
LABORATORY  
ATTN TECHNICAL LIBRARY  
ATTN R. BUSER  
ATTN A. PINTO  
ATTN J. HABERSAT  
FT BELVOIR, VA 22060

COMMANDER  
US ARMY RESEARCH OFFICE  
(DURHAM)  
PO BOX 12211  
ATTN R. J. LONTZ  
ATTN M. STROSIO  
ATTN M. CIFTAN  
ATTN B. D. GUENTHER  
ATTN C. BOGOSIAN  
RESEARCH TRIANGLE PARK, NC  
27709

COMMANDER  
US ARMY RSCH & STD GRP (EUKOPE)  
FPO NEW YORK 09510

COMMANDER  
US ARMY TEST & EVALUATION COMMAND  
ATTN D. H. SLINNEY  
ATTN TECH LIBRARY  
ABERDEEN PROVING GROUND, MD  
21005

DISTRIBUTION (cont'd)

COMMANDER  
US ARMY TROOP SUPPORT COMMAND  
ATTN DRXRES-RTL, TECH LIBRARY  
NATICK, MA 01762

OFFICE OF NAVAL RESEARCH  
ATTN J. MURDAY  
ARLINGTON, VA 22217

DIRECTOR  
NAVAL RESEARCH LABORATORY  
ATTN CODE 2620, TECH LIBRARY BR  
ATTN CODE 5554, F. BARTOLI  
ATTN CODE 5554, L. ESTEROWITZ  
ATTN CODE 5554, R. E. ALLEN  
ATTN L. GOLDBERG  
ATTN M. PARENT  
WASHINGTON, DC 20375

COMMANDER  
NAVAL WEAPONS CENTER  
ATTN CODE 3854, R. SCHWARTZ  
ATTN CODE 3854, M. HILLS  
ATTN CODE 3844, M. NADLER  
ATTN CODE 385, R. L. ATKINS  
ATTN CODE 343, TECHNICAL  
INFORMATION DEPARTMENT  
CHINA LAKE, CA 93555

AIR FORCE OFFICE OF SCIENTIFIC  
RESEARCH  
ATTN MAJOR H. V. WINSOR, USAF  
BOLLING AFB  
WASHINGTON, DC 20332

HQ, USAF/SAMI  
WASHINGTON, DC 20330

DEPARTMENT OF COMMERCE  
NATIONAL BUREAU OF STANDARDS  
ATTN LIBRARY  
WASHINGTON, DC 20234

DIRECTOR  
ADVISORY GROUP ON ELECTRON DEVICES  
ATTN SECTRY, WORKING GROUP D  
201 VARICK STREET  
NEW YORK, NY 10013

AEROSPACE CORPORATION  
PO BOX 92957  
ATTN M. BIRNBAUM  
ATTN N. C. CHANG  
LOS ANGELES, CA 90009

ALLIED  
ADVANCED APPLICATION DEPT  
ATTN A. BUDGOR  
31717 LA TIENDA DRIVE  
WESTLAKE VILLAGE, CA 91362

AMES LABORATORY DOE  
IOWA STATE UNIVERSITY  
ATTN K. A. GSCHNEIDNER, JR. (2 COPIES)  
AMES, IA 50011

ARGONNE NATIONAL LABORATORY  
ATTN W. T. CARNALL  
9700 SOUTH CASS AVENUE  
ARGONNE, IL 60439

BDM CORPORATION  
ATTN R. ATHALE  
MC LEAN, VA 22180

BRIMROSE CORP OF AMERICA  
ATTN R. G. ROSEMEIER  
7527 BELAIR ROAD  
BALTIMORE, MD 21236

CALTECH  
ATTN A. YARIV  
WATSON 128-95  
PASADENA, CA 91125

CORNING GLASS WORKS  
ATTN J. WAHL  
CORNING, NY 14831

ENGINEERING SOCIETIES LIBRARY  
ATTN ACQUISITIONS DEPT  
345 EAST 47TH STREET  
NEW YORK, NY 10017

GTE LABS  
ATTN R. OLSHANSKY  
ATTN U. LANZIERA  
ATTN W. POWAZINIK  
ATTN R. B. LAUER  
40 SYLVAN ROAD  
WALTHAM, MA 02254

IBM RESEARCH DIVISION  
ALMADEN RESEARCH CENTER  
ATTN R. M. MACFARLANE  
MAIL STOP K32 802(D)  
650 HARRY ROAD  
SAN JOSE, CA 95120

DIRECTOR  
LAWRENCE RADIATION LABORATORY  
ATTN M. J. WEBER  
ATTN H. A. KOEHLER  
ATTN W. KRUPKE  
LIVERMORE, CA 94550

MARTIN MARIETTA  
ATTN F. CROWNE  
ATTN R. LEAVITT  
ATTN J. LITTLE  
ATTN T. WORCHESKY

DISTRIBUTION (cont'd)

MARTIN MARIETTA (cont'd)  
ATTN D. WORTMAN  
1450 SOUTH ROLLING ROAD  
BALTIMORE, MD 21227

MIT LINCOLN LAB  
ATTN P. MOULTON,  
ATTN B. AULL  
PO BOX 73  
LEXINGTON, MA 02173

DEPARTMENT OF MECHANICAL, INDUSTRIAL,  
& AEROSPACE ENGINEERING  
ATTN S. TEMKIN  
PO BOX 909  
PISCATAWAY, NJ 08854

NASA/LEWIS RESEARCH CENTER  
ATTN K. BHASIV  
2100 BROOK PARK ROAD  
CLEVELAND, OH 44135

NATIONAL OCEANIC & ATMOSPHERIC ADM  
ENVIRONMENTAL RESEARCH LABS  
ATTN LIBRARY, R-51, TECH RPTS  
BOULDER, CO 80302

OAK RIDGE NATIONAL LABORATORY  
ATTN R. G. HAIRE  
OAK RIDGE, TN 37830

ORTEL CORPORATION  
ATTN K. Y.. LAU  
ATTN B. CHAIM  
ATTN I. URY  
ALHAMBRA, CA 91803

ROME AIR DEVELOPMENT CENTER  
ATTN P. SIRAK  
ATTN B. HENDRICKSON  
ROME, NY

SCIENCE APPLICATIONS, INC  
ATTN T. ALLIK  
1710 GOODRIDGE DRIVE  
McLEAN, VA 22102

UNION CARBIDE CORP  
ATTN M. R. KOKTA  
ATTN J. H. W. LIAW  
750 SOUTH 32ND STREET  
WASHOUGAL, WA 98671

ARIZONA STATE UNIVERSITY  
DEPT OF CHEMISTRY  
ATTN L. EYRING  
TEMPE, AZ 85281

CARNEGIE MELLON UNIVERSITY  
SCHENLEY PARK  
ATTN PHYSICS & EE, J. O. ARTMAN  
ATTN D. CASASANT, B.V.K.V. KUMAR  
PITTSBURGH, PA 15213

COLORADO STATE UNIVERSITY  
PHYSICS DEPARTMENT  
ATTN S. KERN  
FORT COLLINS, CO 80523

DREXEL UNIVERSITY  
DEPT OF ELEC ENGINEERING  
ATTN P. R. HERCZEFELD  
ATTN A. S. DARYOUSH  
PHILADELPHIA, PA 19104

JOHNS HOPKINS UNIVERSITY  
DEPT OF PHYSICS  
ATTN B. R. JUDD  
BALTIMORE, MD 21218

HOWARD UNIVERSITY  
DEPARTMENT OF CHEMISTRY  
ATTN J. NICHOLSON  
ATTN R. BUTCHER  
ATTN M. KRISHNAMURTHY  
WASHINGTON, DC

MASSACHUSETTS INSTITUTE OF  
TECHNOLOGY  
CRYSTAL PHYSICS LABORATORY  
ATTN H. P. JENSSEN  
ATTN A. LINZ  
CAMBRIDGE, MA 02139

MASSACHUSETTS INSTITUTE OF  
TECHNOLOGY  
ATTN V. BAGNATO  
77 MASS AVE  
ROOM 26-251  
CAMBRIDGE, MA 02139

UNIVERSITY OF MARYLAND  
DEPT OF ELECTRICAL ENGINEERING  
ATTN CHI. H. LEE  
ATTN M. DAGENEU  
ATTN RAJ KHANNA (CHEMISTRY)  
COLLEGE PARK, MD

UNIVERSITY OF MICHIGAN  
DEPT OF ELECTRICAL ENGINEERING  
ATTN P. BHATACHARYA  
ATTN J. SINGH  
ATTN G. HADDAD  
ANN ARBOR, MI 48104

DISTRIBUTION (cont'd)

OKLAHOMA STATE UNIVERSITY  
DEPT OF PHYSICS  
ATTN R. C. POWELL  
STILLWATER, OK 74078

PENNSYLVANIA STATE UNIVERSITY  
MATERIALS RESEARCH LABORATORY  
ATTN W. B. WHITE  
ATTN B. K. CHANDRASEKHAR  
UNIVERSITY PARK, PA 16802

SAN JOSE STATE UNIVERSITY  
DEPARTMENT OF PHYSICS  
ATTN J. B. GRUBER  
SAN JOSE, CA 95192

US ARMY LABORATORIES COMMAND  
ATTN TECHNICAL DIRECTOR, AMSLC-CT

INSTALLATION SUPPORT ACTIVITY  
ATTN LEGAL OFFICE, SLCIS-CC  
ATTN S. ELBAUM, SLCIS-CC-IP

USAISC  
ATTN RECORD COPY, ASNC-LAB-TS  
ATTN TECHNICAL REPORTS BRANCH,  
ASNC-LAB-TR (2 COPIES)

HARRY DIAMOND LABORATORIES  
ATTN D/DIVISION DIRECTORS  
ATTN LIBRARY, SLCHD-TL (3 COPIES)  
ATTN LIBRARY, SLCHD-TL (WOODBIDGE)  
ATTN CHIEF, SLCHD-NW-E  
ATTN CHIEF, SLCHD-NW-EP  
ATTN CHIEF, SLCHD-NW-EH  
ATTN CHIEF, SLCHD-NW-ES  
ATTN CHIEF, SLCHD-NW-R  
ATTN CHIEF, SLCHD-NW-TN  
ATTN CHIEF, SLCHD-NW-RP  
ATTN CHIEF, SLCHD-NW-CS  
ATTN CHIEF, SLCHD-NW-TS  
ATTN CHIEF, SLCHD-NW-RS  
ATTN CHIEF, SLCHD-NW-P  
ATTN CHIEF, SLCHD-PO  
ATTN CHIEF, SLCHD-ST-C  
ATTN CHIEF, SLCHD-ST-AP

HARRY DIAMOND LABORATORIES (cont'd)  
ATTN CHIEF, SLCHD-ST-OP  
ATTN CHIEF, SLCHD-ST-RS  
ATTN CHIEF, SLCHD-ST-SS  
ATTN CHIEF, SLCHD-TT  
ATTN WALTER, SANDRA, SLCIS-CP-TD  
ATTN WILLIS, B., SLCHD-IT-EB  
ATTN ZABLUDOWSKI, B., SLCHD-IT-EB  
ATTN HERSHALL, P., SLCHD-MI-S  
ATTN KENYON, C. S., SLCHD-NW-EP  
ATTN MILETTA J. R., SLCHD-NW-EP  
ATTN McLEAN, F. B., SLCHD-NW-RP  
ATTN SATTLER, J., SLCHD-PO-P  
ATTN LIBELO, L., SLCHD-ST-MW  
ATTN BENCIVENGA, A. A., SLCHD-ST-RP  
ATTN NEMARICH, J., SLCHD-ST-SP  
ATTN WEBER, B., SLCHD-ST-R  
ATTN BAHDER, T., SLCHD-ST-AP  
ATTN BRODY, P., SLCHD-ST-AP  
ATTN BRUNO, J., SLCHD-ST-AP  
ATTN DROPKIN, H., SLCHD-ST-AP  
ATTN EDWARDS, SLCHD-ST-AP  
ATTN HANSEN, A., SLCHD-ST-AP  
ATTN HAY, G., SLCHD-ST-AP  
ATTN KATZEN, E., SLCHD-ST-AP  
ATTN MORRISON, C., SLCHD-ST-AP  
ATTN NEIFELD, R., SLCHD-ST-AP  
ATTN PENNISE, C., SLCHD-ST-AP  
ATTN SCHMALBACH, R., SLCHD-ST-AP  
ATTN SIMONIS, G., SLCHD-ST-AP  
ATTN STEAD, M., SLCHD-ST-RP  
ATTN STELLATO, J., SLCHD-ST-AP  
ATTN TOBIN, M., SLCHD-ST-AP  
ATTN TOBER, R., SLCHD-ST-AP  
ATTN TURNER, G., SLCHD-ST-AP  
ATTN WONG, B., SLCHD-ST-AP  
ATTN WORTMAN, D., SLCHD-ST-AP  
ATTN GARVIN, C., SLCHD-ST-OP  
ATTN GUPTA, N., SLCHD-ST-OP  
ATTN MASLOWE, B., SLCHD-ST-OP  
ATTN HARRISON, L., SLCHD-ST-OP  
ATTN SCHOCKLEY, D., SLCHD-ST-OP  
ATTN GOFF, J., SLCHD-ST-SS  
ATTN BENCIVENGA B., SLCHD-TA-AS  
ATTN SEMENDY, F., SLCHD-ST-OP (20 COPIES)